Commun. Theor. Phys. **75** (2023) 125404 (14pp) https://doi.org/10.1088/1572-9494/ad0e05

Particle dynamics, black hole shadow and weak gravitational lensing in the $f(Q)$ theory of gravity

Allah Ditta[1], Xia Tiecheng[1], Farruh Atamurotov[2,3,4,5], Ibrar Hussain[6,*] and G Mustafa[7]

[1] Department of Mathematics, Shanghai University and Newtouch Center for Mathematics of Shanghai University, Shanghai, 200444, Shanghai, China
[2] New Uzbekistan University, Movarounnahr Street 1, Tashkent 100000, Uzbekistan
[3] Central Asian University, Milliy Bog' Street 264, Tashkent 111221, Uzbekistan
[4] Tashkent University of Applied Sciences, Str. Gavhar 1, Tashkent 100149, Uzbekistan
[5] Institute of Theoretical Physics, National University of Uzbekistan, Tashkent 100174, Uzbekistan
[6] School of Electrical Engineering and Computer Science, National University of Sciences and Technology, H-12, Islamabad, Pakistan
[7] Department of Physics, Zhejiang Normal University, Jinhua 321004, China

E-mail: mradshahid01@gmail.com, xiatc@shu.edu.cn, atamurotov@yahoo.com, ibrar.hussain@seecs.nust.edu.pk and gmustafa3828@gmail.com

Received 1 August 2023, revised 7 November 2023
Accepted for publication 20 November 2023
Published 20 December 2023

Abstract

We study the particle dynamics around a black hole (BH) in $f(Q)$ gravity. First, we investigate the influence of the parameters of $f(Q)$ gravity on the horizon structure of the BH, photon orbits and the radius of the innermost stable circular orbit (ISCO) of massive particles. We further study the effects of the parameters of $f(Q)$ gravity on the shadow cast by the BH. Moreover, we consider weak gravitational lensing using the general method, where we also explore the deflection angle of light rays around the BH in $f(Q)$ gravity in uniform and nonuniform plasma mediums.

Keywords: *f(Q)* gravity, black holes, photon motion, shadow and lensing

(Some figures may appear in colour only in the online journal)

1. Introduction

General relativity (GR) was proposed by Einstein in 1915 as a basic theory that explains the nature of the fundamental force of gravity. The Einstein theory of gravity has successfully passed the test based on different observations and experiments on a macroscopic scale in the Universe. Applying GR can be counted as an examination in the weak field regime to test it within the solar system [1], and it has already been done. The current scrutiny about gravitational waves [2] and the shadows of M87* and SgrA* [3, 4] can be counted as an examination of GR in the dexterous field regime. The theory of GR during gravitational collapse has some limitations in explaining the features of the singularity. Other issues that cannot be well explained in the framework of GR include the rotation curve of galaxies, cosmic acceleration, dark energy/matter and the quantum theory of gravity. To resolve these issues, it has been suggested by different authors that the theory of GR should be amended.

Symmetric teleparallelism (ST) is a generalization of GR, which is differentiated from GR based on different sets of geometric postulates. The affine connection, $\Gamma^{\alpha}_{\mu\nu}$, plays a vital role in differentiating the theory of GR from ST. In GR, the connection is supposed to be torsion-free and metric-compatible, which means it is genuinely based on the Levi-Civita connection. Metric-compatibility hypothesis in ST is excluded and in place of it $\Gamma^{\alpha}_{\mu\nu}$ becomes torsion-free and results into a vanishing Riemann curvature tensor. As for how this

* Author to whom any correspondence should be addressed.

connection fulfills these hypotheses, it can be understood as becoming independent of the metric in a specific and arbitrary manner. Along with the curvature and torsion of $\Gamma^{\alpha}_{\mu\nu}$ taken as zero, only the non-metricity tensor $\mathcal{Q}_{\alpha\mu\nu}$ is the non-trivial object in ST which is responsible for defining the affine geometry. Non-metricity scalar Q defines the action of ST and can be calculated by using the non-metricity tensor, $\mathcal{Q}_{\alpha\mu\nu}$. Famously, the action of ST to a boundary term has a close approximation to the Einstein–Hilbert action of GR [5–9]. Therefore, the geometric description of symmetric teleparallel gravity (STG) is different from GR. Specifically, it can be shown that the appearance of only affine connection as a boundary term in the action is non-physical. In short, the field equations are totally independent of the choice of connection, and any connection having compatibility with the STG can be chosen in the field equations. Thus the physical degree of freedom is purely metric-dependent and any sort of connection does not hold any form of physical information.

Changes may occur while taking the generalizations to the more generic theories which are quadratic in the non-metricity tensor [10], or an expansion of STG [11]. In this manuscript, we are interested in the non-linear extension defined by the action: $\int \mathrm{d}^4x\sqrt{-g}f(Q)$ [5], where $f(Q)$ shows the prior arbitrary function of Q. This theory not only possesses non-equivalence to $f(R)$ gravity, but also considers the degree of freedom based on the affine connection. The dependence on $\Gamma^{\alpha}_{\mu\nu}$ should not be further absorbed into a boundary term in the action. It can be expected that the connection will influence the metric defining the gravity. Against the claim present in the literature [12, 13], we work with the realization of this expectation [14] by studying the most common version of static and spherically symmetric spacetimes incorporated in the $f(Q)$ theory of gravity.

Test particle motion can be studied as a beneficial tool to examine the metric-based theories defining gravity as a spacetime structure. The impacts of the spacetime curvature and gravitational field parameters on the particle motion have been extensively studied in the literature [15–30]. Analyzing the motion of test particles having non-vanishing electric and magnetic charge may lead towards a direct understanding of the essence of the gravitational and electromagnetic field around the gravitating compact object. Knowledge of photon motion in the vicinity of compact objects, like BHs, is essential for studying the gravitational lensing and shadows cast by BHs and can enhance our understanding about different structures, like distant galaxies, in the Universe. Gravitational lensing can be divided into two categories: (a) strong gravitational lensing with the gravitational deflection angle considerably larger than one and (b) weak gravitational lensing with the gravitational deflection angle considerably less than one. It is assumed that weak gravitational lensing can be considered in investigating the cause of the current accelerated expansion of the cosmos [31]. Astrophysically, the observed bending of light and gravitational lensing fall in the limit of weak gravitational lensing, i.e. with the deflection angles very much less than one [32]. Therefore, the study of weak gravitational lensing is even more fascinating. Furthermore, it is of much interest to study the gravitational lensing in a plasma medium as it is assumed that the light rays in space always travel through such mediums (see more examples [33–50] and other works [51–54]). In a field having nonuniform plasma, photons travel along curved trajectories, since plasma is a medium possessing a dispersive property, having a permittivity tensor based on its density [55]. Photon trajectory in a dispersive nonuniform plasma medium is based on the frequency of the photon without any relation to the gravity. The photon deflection in a nonuniform plasma with the presence of gravity has been discussed in the literature [56, 57]. This study considers a linear approximation with two effects independently: (a) the deflection caused by the gravitation in the vacuum and (b) the deflection caused as a result of the non-homogeneity of the medium. The first effect is neutral and the second effect is based upon the frequency of photon in a dispersive medium and it approaches to zero in a homogeneous medium. The study of the shadow cast by a BH may provide useful insight on estimation of the value of the spin parameter of a rotating BH [58–60]. The BH shadow with and without plasma has been analysed for different BHs in the literature [61–88].

Almost one hundred years after the initial observation of gravitational light deflection, in 2019 a significant breakthrough happened, when the Event Horizon Telescope (EHT) Collaboration [4] accomplished a momentous feat by predicting an image of a BH. This achievement stemmed from our understanding that, when light closely approaches a BH, it shows observable deflection, occasionally traversing circular orbits. This considerable light deflection, combined with the intrinsic property that no light escapes from a BH, leads to the hypothesis of a dark disk-like region inside the celestial sphere, known as the BH shadow. The concept of observing this shadow was first hypothesized in the year 2000 [60], which was later acknowledged by the authors in reference [89], through continuous numerical simulations, suggesting the conclusion that successful observations could be made at wavelengths near 1 mm using the technique of very long baseline interferometry (VLBI). The recent remarkable achievement of the EHT Collaboration motivated us to deepen our understanding and provide explanations for both what we can observe and what remains concealed [90].

In this work, we discuss the motion of particles, the BH shadow and weak gravitational lensing in the presence of plasma in $f(Q)$ gravity to look at the effects of the parameters present in $f(Q)$ gravity and get some new insights about this alternative theory of gravity. In section 2 we discuss the basics of $f(Q)$ gravity and particle dynamics. In section 2.1, we study massive particle motion, and section 2.2 consists of the discussion about the motion of massless particles around a BH in $f(Q)$ gravity. Section 3 contains a discussion of BH shadows in $f(Q)$ gravity. In section 4, we investigate weak gravitational lensing (section 4.1 for uniform plasma, and section 4.2 for nonuniform plasma) in the $f(Q)$ theory of gravity. In section 5, we present the conclusion for our study. Throughout we use a system of units in which $G = 1 = c$.

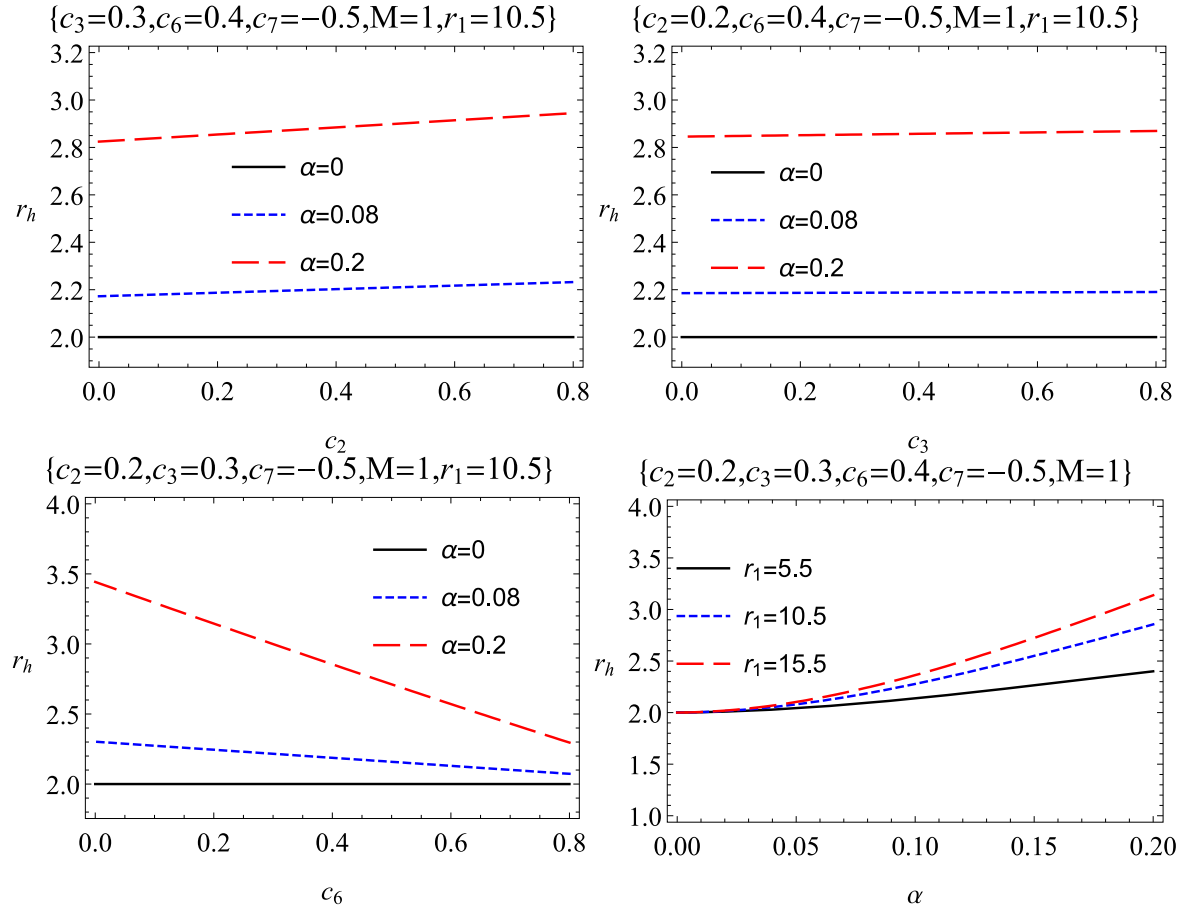

Figure 1. Dependence of the horizon structure on $f(Q)$ parameters.

2. Particle motion around a black hole in $f(Q)$ gravity

In this study we consider the action for $f(Q)$ gravity [14], given by

$$S = \int \sqrt{-g}\mathrm{d}^4x\left[\frac{1}{2}f(Q) + \lambda_{\xi}^{\beta\mu\nu}R_{\beta\mu\nu}^{\xi} + \lambda_{\xi}^{\mu\nu}T_{\mu\nu}^{\xi} + L_m\right], \quad (1)$$

where the determinant of $g_{\mu\nu}$ is denoted by g, $f(Q)$ is the function of non-metricity Q, $\lambda_{\xi}^{\beta\mu\nu}$ is the multiplier for the Lagrangian, and L_m denotes the matter Lagrangian density. The metric components in their complete format can be put in the following form [14]

$$g_{tt} = -\left(1 - \frac{2M_{\text{ren}}}{r}\right) + \alpha^2\frac{\mu}{r}\ln\left(\frac{r}{r_1}\right),$$
$$g_{rr} = -\frac{1}{g_{tt}}, \quad (2)$$

where M_{ren} is the renormalized mass which is given by

$$2M_{\text{ren}} := 2M + \alpha\, c_2 + \alpha^2(c_3 - 16M^2(3c_6 + c_7)), \quad (3)$$

where the above equation satisfies the field equations of the theory under consideration. The scale r_1 can be initiated by the change in the constant like $c_6 \to c_6 - 48M^2c_7\ln(r_1)$, in a desire to have a dimension-free argument in the logarithm function. Here, we describe a new scale

$$\mu := 48\, M^2\, c_7, \quad (4)$$

whose strength is characterized beyond the GR correction, which is another new 'BH charge', also known as connection hair. It is worth taking into consideration that the correction terms could accelerate deviations from the Schwarzschild solution for larger values of r. The correction term for the logarithm will be determined by the command for radii upon the renormalized Schwarzschild term, satisfying the relation

$$|\ln(r/r_1)| > \frac{2M_{\text{ren}}}{\alpha^2|\mu|}. \quad (5)$$

All the $f(Q)$ setup is based upon the model $f(Q) = Q + \alpha Q^2$, so α is a constant parameter with real values. In order to produce results very close to the theory of GR, as an ansatz we set $|\alpha| \ll 1$. c_i is a real integration constant. The above equation (5) expresses the breakdown of the perturbation theory at larger values of r. Metric perturbations are small exclusively at the smaller values of r in comparison to the background of the Schwarzschild spacetime. The increasing and decreasing behavior of the horizon structure of the BH in $f(Q)$ gravity can be seen in figure 1 and is calculated using the condition $g_{tt} = f(r) = 0$. It can be noticed that one can retrieve the Schwarzschild case by replacing $\alpha = 0$ in equation (2). From figure 1, one can notice that the horizon

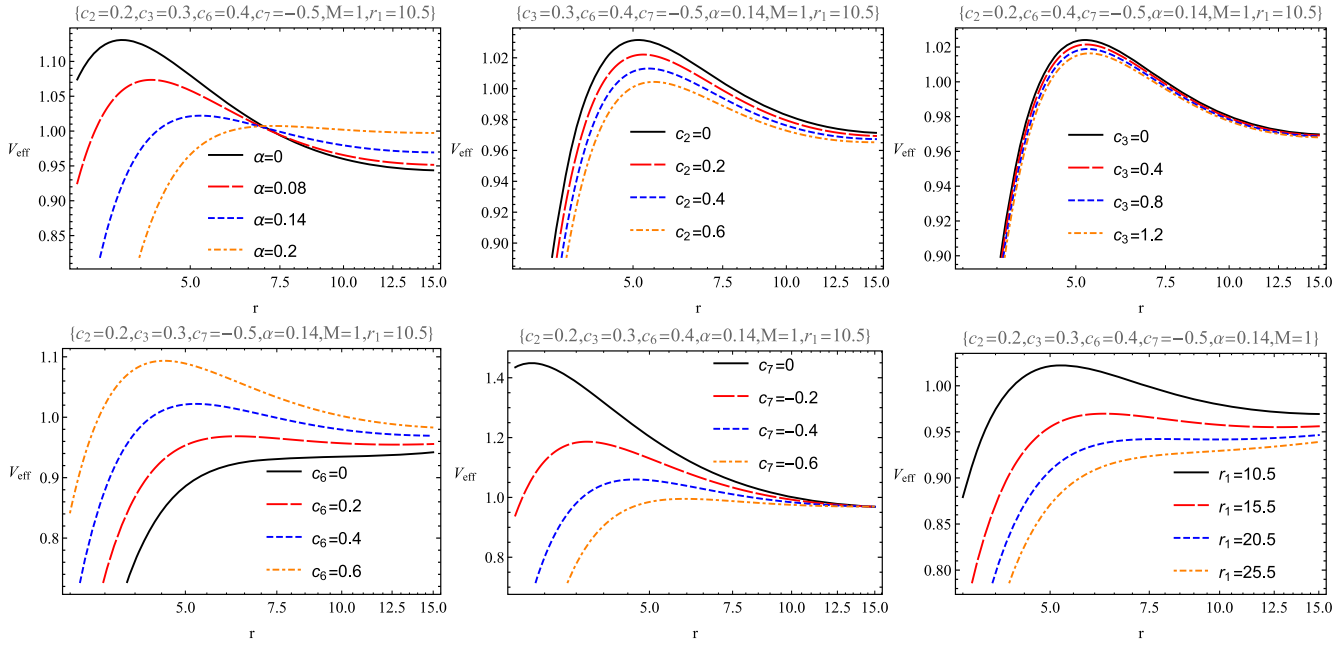

Figure 2. $V_{\rm eff}$ along radial coordinate r of the massive particle.

radius for the $f(Q)$ BH considered in the present study is bigger than that of the Schwarzschild BH.

For the next two subsections we will discuss the massive and massless particles motion in the vicinity of a BH in $f(Q)$ gravity:

2.1. Massive particle motion around a black hole in f(Q) gravity

The trajectory of the test particle can be found by taking into account the Lagrangian for the test particle having mass m in the form given below

$$\mathcal{L}' = \frac{1}{2} g_{\mu\nu} u^\mu u^\nu, \quad u^\mu = \frac{{\rm d}x^\mu}{{\rm d}\tau}, \tag{6}$$

where τ represents an affine parameter, x^μ denotes the coordinates and u^μ expresses the four-velocity of the test particle. The conserved quantities responsible for the motion of the test particle, such as the energy $\mathcal{E}$ and the angular momentum $\mathcal{L}$, can be put in the form below:

$$\mathcal{E} = \frac{\partial \mathcal{L}'}{\partial u^t} = -f(r)\frac{{\rm d}T}{{\rm d}\tau},$$
$$\mathcal{L} = \frac{\partial \mathcal{L}'}{\partial u^\phi} = r^2 \sin^2\theta \frac{{\rm d}\phi}{{\rm d}\tau}. \tag{7}$$

If we put equation (7) into the normalization condition $g_{\mu\nu}u^\mu u^\nu = -\epsilon$, it is very convenient to find the equations of motion of a test particle in the equatorial plane in which we have $\theta = \frac{\pi}{2}$ as [91]:

$$\frac{{\rm d}r}{{\rm d}\tau} = \sqrt{\mathcal{E}^2 - f(r)(\epsilon + \frac{\mathcal{L}^2}{r^2})}, \tag{8}$$

$$\frac{{\rm d}\phi}{{\rm d}\tau} = \frac{\mathcal{L}^2}{r^2}, \tag{9}$$

$$\frac{{\rm d}t}{{\rm d}\tau} = \frac{\mathcal{E}}{f(r)}, \tag{10}$$

where parameter ϵ is described as given below [91]:

$$\epsilon = \begin{cases} 1, & \text{for timelike geodesics} \\ 0, & \text{for null geodesics} \\ -1, & \text{for spacelike geodesics} \end{cases}. \tag{11}$$

The equation expressing the radial motion reduces into the following specific form:

$$\left(\frac{{\rm d}r}{{\rm d}\tau}\right)^2 = \mathcal{E}^2 - V_{\rm eff}(r) = \mathcal{E}^2 - f(r)\left(1 + \frac{\mathcal{L}^2}{r^2}\right), \tag{12}$$

where

$$V_{\rm eff}(r) = f(r)\left(1 + \frac{\mathcal{L}^2}{r^2}\right). \tag{13}$$

Here, $V_{\rm eff}(r)$ represents the effective potential for the motion of the test particles. For a massive test particle, the effective potential depends on the radial coordinate around the BH. For some different values of the parameters α, c_2, c_3, c_6, c_7 and r_1 which can be fixed for the correct depiction of results, is shown in figure 2. It shows that the stable circular orbits move with respect to the central compact object. Moreover, $V_{\rm eff}(r)$ for the current study is less than the Schwarzschild case, where $\alpha = 0$.

One can use the conditions $\dot{r} = 0$ and ${\rm d}\dot{r} = 0$ to discuss the circular motion of a neutral particle around the BH in $f(Q)$ gravity. These conditions permit one to get an expression for the energy $\mathcal{E}$ and also for the angular momentum $\mathcal{L}$ of the test particle in the equations

$$\mathcal{L}^2 = \frac{1}{3} r^2((96\alpha^2 c_7 M^2 - 2r)(3\alpha(c_2 + \alpha c_3)$$
$$+6M(1 - 8\alpha^2 M(3c_6 + 2c_7))$$
$$+144\alpha^2 c_7 M^2(\ln(r) - \ln(r_1)) - 2r)^{-1} - 1), \tag{14}$$

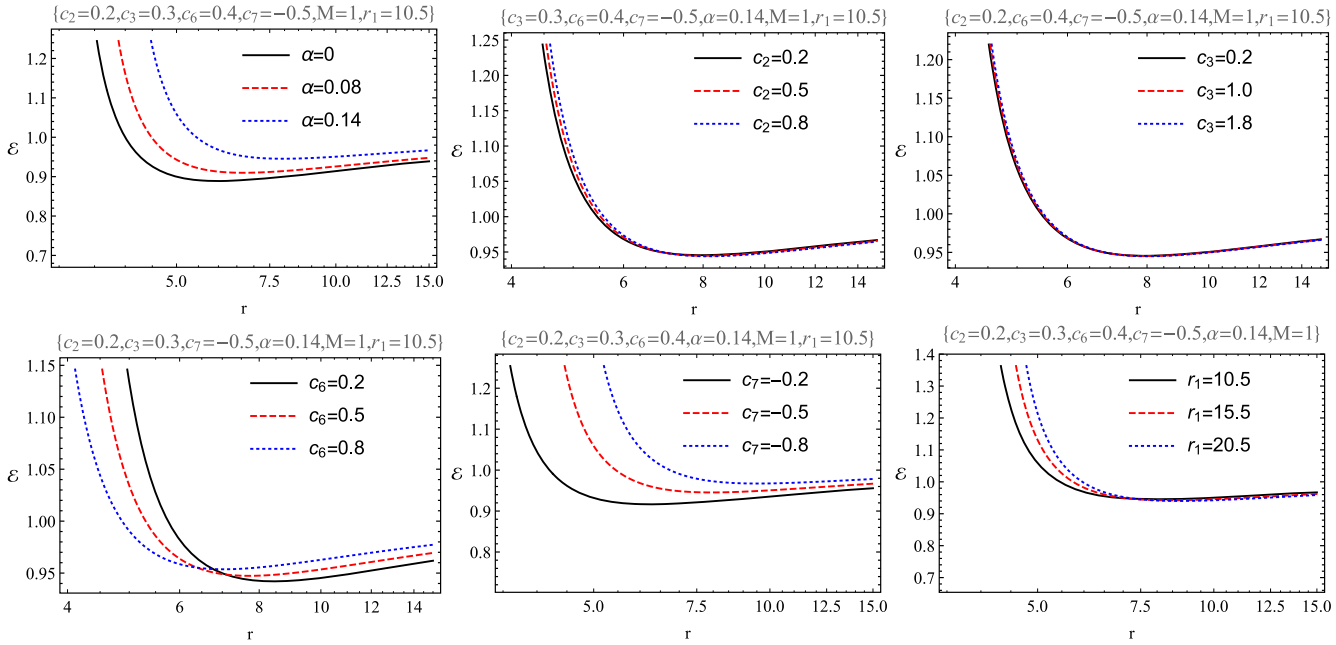

Figure 3. $\mathcal{E}$ along the radial coordinate r of the massive particle.

and

$$\mathcal{E}^2 = \frac{(-\alpha(c_2+\alpha c_3)+2M(8\alpha^2M(3c_6+c_7)-1)-48\alpha^2c_7M^2(\ln(r)-\ln(r_1))+r)J_1(r)}{3r}, \tag{15}$$

where

$$J_1(r) = \left(\frac{2(r-48\alpha^2c_7M^2)}{-3\alpha(c_2+\alpha c_3)+6M(8\alpha^2M(3c_6+2c_7)-1)+144\alpha^2c_7M^2(\ln(r_1)-\ln(r))+2r}+2\right).$$

Further detailed information regarding the conserved quantities can be obtained from the graphs presented in figures 3 and 4. These graphs show the shift of the curves with respect to the central BH for parameters α, c_2, c_3, c_6, c_7 and r_1 of $f(Q)$ gravity. Also, $\mathcal{E}$ and $\mathcal{L}$ in our present study are more than the GR case, where $\alpha = 0$.

Now, we may take into consideration the radius of the ISCO, r_{ISCO}. In order to calculate r_{ISCO}, we have to utilize the following conditions [91]:

$$\begin{aligned} V'_{\text{eff}} &= 0, \\ V''_{\text{eff}} &= 0. \end{aligned} \tag{16}$$

Due to the complexity of the system we cannot deal with r_{ISCO} analytically. The detailed behaviour of the ISCO depending upon the parameters c_2, c_3, c_6, c_7 and r_1 is shown in figure 5. In particualr, one can see that r_{ISCO} is bigger than the GR case ($\alpha = 0$), and increases with the parameters c_2, c_6 and α, and decreases with the parameter c_7.

2.2. Massless particle motion around a black hole in f(Q) gravity

In this subsection, we study the massless particle (photon) motion in a BH spacetime in $f(Q)$ gravity. By utilizing the metric Lagrangian of the $f(Q)$ gravity BH spacetime, one can obtain the equation of photon motion around the BH in the $f(Q)$ theory of gravity by taking $\epsilon = 0$ in equation (11). In the equatorial plane the equation of motion can be represented as follows:

$$\dot{r}^2 = \mathcal{E}^2 - f(r)\frac{\mathcal{L}^2}{r^2}, \tag{17}$$

$$\dot{\phi} = \frac{\mathcal{L}}{r^2}, \tag{18}$$

$$\dot{t} = \frac{\mathcal{E}}{f(r)}. \tag{19}$$

By utilizing equation (17), one can easily get the expression for effective potential V_{eff} of the motion of the photon as [91]:

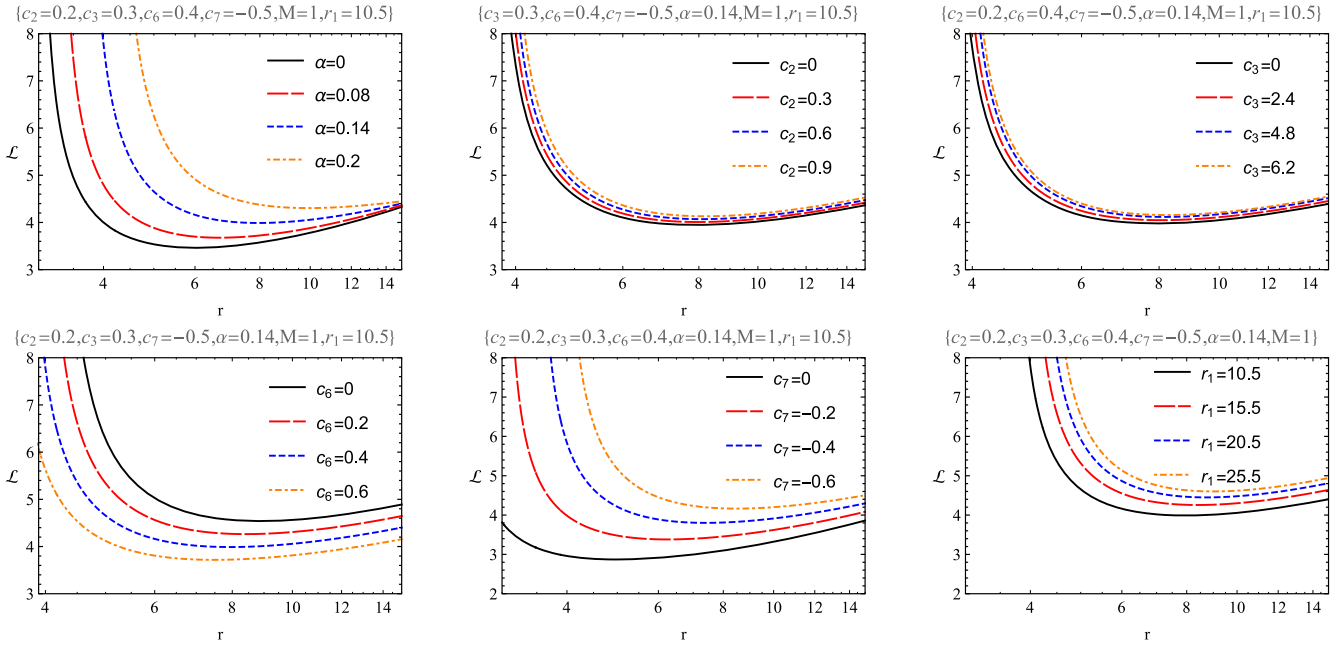

Figure 4. $\mathcal{L}$ along the radial coordinate r of the massive particle.

$$V_{\text{eff}} = f(r)\frac{\mathcal{L}^2}{r^2}. \tag{20}$$

Effective potential dependence on the radial coordinate for the motion of photons is given in figure 6. The shift of photon orbit towards and outwards from the central object for different parameters can be seen in figure 6. The photon's circular orbit radius r_{ph} around the BH in $f(Q)$ gravity can be obtain from the solution of the second equation given in equation (16). Being complex, we deal with it numerically. The increasing and decreasing behaviour of the photon circular orbits r_{ph} with the $f(Q)$ gravity parameters c_2, c_3, c_6, c_7, r_1 and α is expressed in figure 7. Notice that the increasing and decreasing trend of the radius of the photon orbits is similar to that for the massive particle discussed above.

3. Black hole shadow in $f(Q)$ gravity

This section consists of the study of BH shadows in the $f(Q)$ theory of gravity. The angular radius of the BH shadow [61, 83] consists of the following expression:

$$\sin^2\alpha_{\text{sh}} = \frac{Y(r_{\text{ph}})^2}{Y(r_{\text{obs}})^2}, \tag{21}$$

with

$$Y(r)^2 = \frac{g_{22}}{g_{00}} = \frac{r^2}{f(r)}, \tag{22}$$

where α_{sh} denotes the angular radius of the BH shadow, r_{obs} represents the observed distance and r_{ph} stands for the radius of the photon sphere. By combining equations (21) and (22), we obtain the following relation

$$\sin^2\alpha_{\text{sh}} = \frac{r_{\text{ph}}^2}{f(r_{\text{ph}})}\frac{f(r_{\text{obs}})}{r_{\text{obs}}^2}. \tag{23}$$

By utilizing equation (23), the radius of the BH shadow at a large distance for an observer can conveniently be found [61]:

$$R_{\text{sh}} \simeq r_{\text{obs}}\sin\alpha_{\text{sh}} \simeq \frac{r_{\text{ph}}}{\sqrt{f(r_{\text{ph}})}}. \tag{24}$$

Finally, equation (24) is the non-rotating case of the shadow of the BH. Figure 8 is the graphical depiction of the radius of the BH shadow in $f(Q)$ gravity for various values of the parameters involved. It is important to notice that the BH shadow decreases as compared to the Schwarzschild BH shadow, indicated by the black solid line (curve) along the increasing values of c_6. Furthermore, we notice that the shadow of the BH in $f(Q)$ gravity increases with the increase in the values of the parameters c_2, c_3 and α.

4. Weak gravitational lensing in $f(Q)$ gravity

In this section, we study an optical characteristic of the BH in $f(Q)$ gravity by analysing the effect of weak gravitational lensing. For an approximation to the weak field, the following form of the metric tensor [33, 34] can be used:

$$g_{\alpha\beta} = \eta_{\alpha\beta} + h_{\alpha\beta}, \tag{25}$$

where $\eta_{\alpha\beta}$ and $h_{\alpha\beta}$ denote the Minkowski spacetime and the perturbed gravitational field describes the $f(Q)$ theory of gravity. The following properties are essential for the two

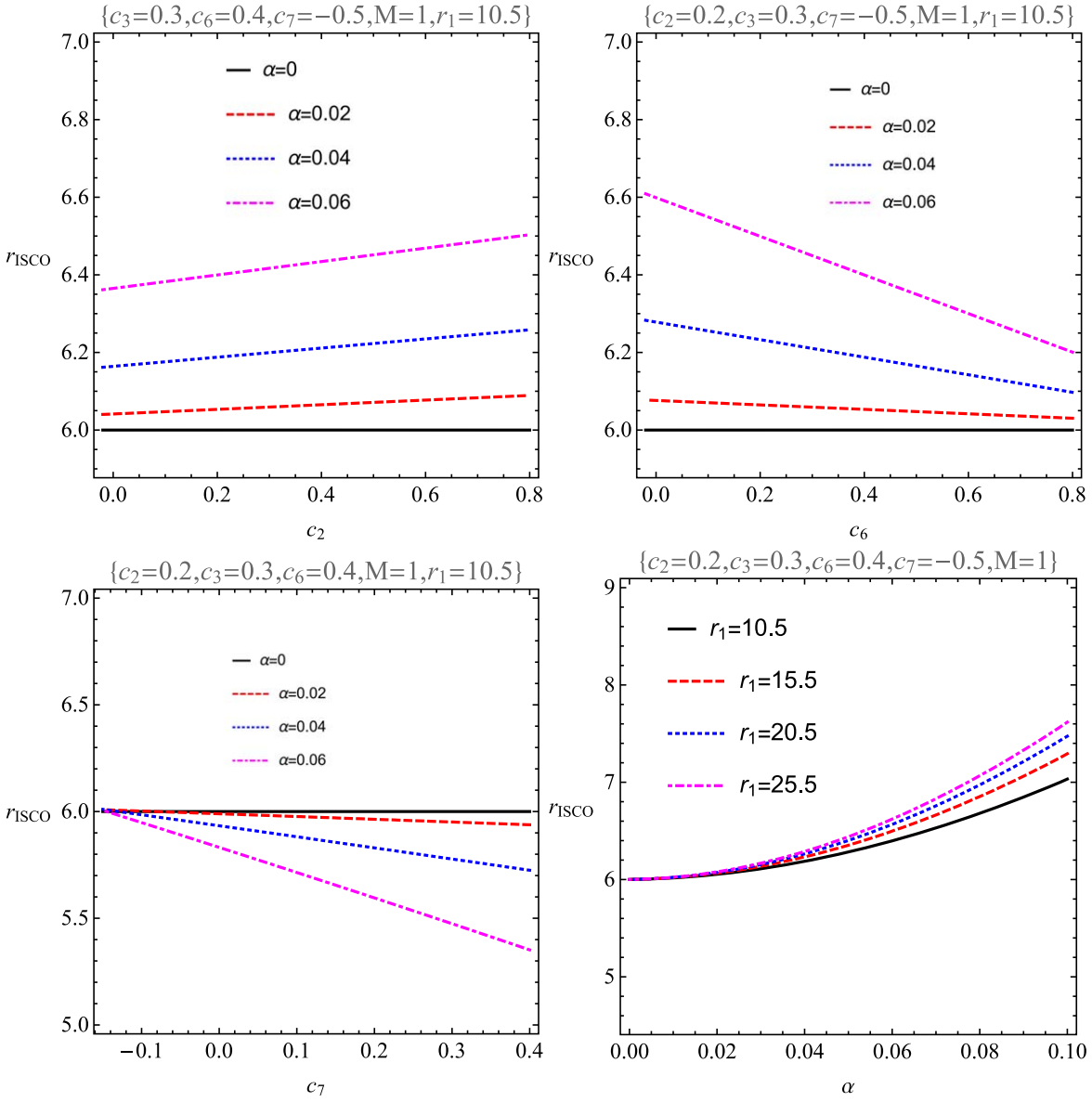

Figure 5. r_{ISCO} with parameters c_2, c_6, c_7 and α for different values of α and r_1.

terms $\eta_{\alpha\beta}$ and $h_{\alpha\beta}$

$$\begin{aligned}&\eta_{\alpha\beta} = \text{diag}(-1,\,1,\,1,\,1),\\&h_{\alpha\beta} \ll 1, \quad h_{\alpha\beta} \to 0 \quad \text{under} \quad x^i \to \infty,\\&g^{\alpha\beta} = \eta^{\alpha\beta} - h^{\alpha\beta}, \quad h^{\alpha\beta} = h_{\alpha\beta}.\end{aligned} \tag{26}$$

The general equation of the angle of deflection in the presence of a plasma medium can be written in the following form [33, 34]

$$\hat{\alpha}_i = \frac{1}{2}\int_{-\infty}^{\infty}\left(h_{33} + \frac{h_{00}\omega^2 - K_e N(x^i)}{\omega^2 - \omega_e^2}\right)_{,i} \mathrm{d}z,\; i = 1,\,2, \tag{27}$$

where $N(x^i)$ is the density of the plasma particles around the BH, $K_e = 4\pi e^2/m_e$ is a constant, and ω and $\omega_e = 4\pi e^2 N(x^i)/m = K_e N(x^i)$ are photon and plasma frequencies, respectively [33]. By the use of the basic equations (27)–(26), we arrive at the expression for the angle of deflection around the BH in $f(Q)$ gravity, as given below [33]:

$$\hat{\alpha}_{\mathrm{b}} = \frac{1}{2}\int_{-\infty}^{\infty}\frac{b}{r}\left(\frac{\mathrm{d}h_{33}}{\mathrm{d}r} + \frac{1}{1-\omega_e^2/\omega}\frac{\mathrm{d}h_{00}}{\mathrm{d}r} - \frac{K_e}{\omega^2-\omega_e^2}\frac{\mathrm{d}N}{\mathrm{d}r}\right)\mathrm{d}z. \tag{28}$$

The metric element can be rewritten in the below given form:

$$\begin{aligned}\mathrm{d}s^2 = \mathrm{d}s_0^2 &+ \left(\alpha^2 c_7 M^2 \ln\left(\frac{r}{r_1}\right) + \frac{2M_{\mathrm{ren}}}{r}\right)\mathrm{d}t^2\\&+ \left(\alpha^2 c_7 M^2 \ln\left(\frac{r}{r_1}\right) + \frac{2M_{\mathrm{ren}}}{r}\right)\mathrm{d}r^2,\end{aligned} \tag{29}$$

where $\mathrm{d}s_0^2 = -\mathrm{d}t^2 + \mathrm{d}r^2 + r^2(\mathrm{d}\theta^2 + \sin^2\theta\mathrm{d}\phi^2)$.

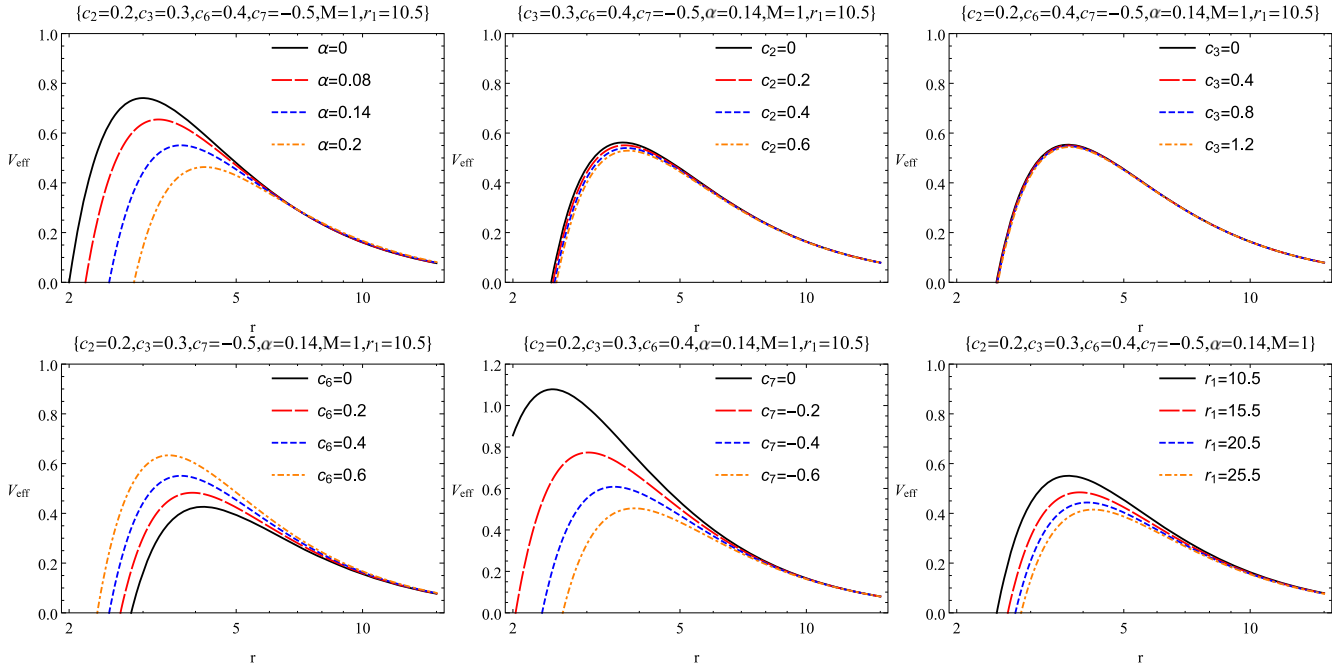

Figure 6. V_{eff} and the radial coordinate r of the massless particle.

It is convenient to find the components $h_{\alpha\beta}$ of the metric in the form of Cartesian coordinates:

$$h_{00} = \left(-\frac{\alpha^2 c_3}{r} - \frac{\alpha c_2}{r} - \frac{9\alpha^2 c_7 R_s^2 \ln\left(\frac{r}{r_1}\right)}{r} + \frac{12\alpha^2 c_6 R_s^2}{r} + \frac{4\alpha^2 c_7 R_s^2}{r} - \frac{R_s}{r}\right), \tag{30}$$

$$h_{ik} = \left(-\frac{\alpha^2 c_3}{r} - \frac{\alpha c_2}{r} - \frac{9\alpha^2 c_7 R_s^2 \ln\left(\frac{r}{r_1}\right)}{r} + \frac{12\alpha^2 c_6 R_s^2}{r} + \frac{4\alpha^2 c_7 R_s^2}{r} - \frac{R_s}{r}\right) n_i n_k, \tag{31}$$

$$h_{33} = \left(-\frac{\alpha^2 c_3}{r} - \frac{\alpha c_2}{r} - \frac{9\alpha^2 c_7 R_s^2 \ln\left(\frac{r}{r_1}\right)}{r} + \frac{12\alpha^2 c_6 R_s^2}{r} + \frac{4\alpha^2 c_7 R_s^2}{r} - \frac{R_s}{r}\right) \cos^2\chi, \tag{32}$$

where $\cos^2\chi = z^2/(b^2+z^2)$ and $r^2 = b^2 + z^2$ [33].

Differentiation of h_{00} and h_{33} with respect to the radial coordinate is described by:

$$\frac{dh_{00}}{dr} = \frac{\alpha^2 c_3}{r^2} + \frac{\alpha c_2}{r^2} + \frac{9\alpha^2 c_7 R_s^2 \ln\left(\frac{r}{r_1}\right)}{r^2} - \frac{12\alpha^2 c_6 R_s^2}{r^2} - \frac{13\alpha^2 c_7 R_s^2}{r^2} + \frac{R_s}{r^2}, \tag{33}$$

$$\frac{dh_{33}}{dr} = \frac{3z^2\left(\alpha^2 c_3 + \alpha c_2 + R_s\left(\alpha^2 c_7 R_s\left(9\ln\left(\frac{r}{r_1}\right) - 7\right) - 12\alpha^2 c_6 R_s + 1\right)\right)}{r^4}. \tag{34}$$

The following is the relation representing the deflection angle [40]

$$\hat{\alpha}_b = \hat{\alpha}_1 + \hat{\alpha}_2 + \hat{\alpha}_3, \tag{35}$$

where

$$\hat{\alpha}_1 = \frac{1}{2}\int_{-\infty}^{\infty} \frac{b}{r}\frac{dh_{33}}{dr}\,dz,$$
$$\hat{\alpha}_2 = \frac{1}{2}\int_{-\infty}^{\infty} \frac{b}{r}\frac{1}{1-\omega_e^2/\omega}\frac{dh_{00}}{dr}\,dz,$$
$$\hat{\alpha}_3 = \frac{1}{2}\int_{-\infty}^{\infty} \frac{b}{r}\left(-\frac{K_e}{\omega^2-\omega_e^2}\frac{dN}{dr}\right)dz. \tag{36}$$

Now we make a schematic plan to analyse and calculate the deflection angle for different forms of the plasma density distributions.

4.1. Uniform plasma distribution

The gravitational deflection angle around the BH in $f(Q)$ gravity containing uniform plasma is written in the form of the following relation [40]:

$$\hat{\alpha}_{\rm uni} = \hat{\alpha}_{\rm uni1} + \hat{\alpha}_{\rm uni2} + \hat{\alpha}_{\rm uni3}. \tag{37}$$

By using equations (32), (35) and (36), it is easy to obtain the expression for the deflection angle around the BH in $f(Q)$ gravity in a medium consisting of uniform plasma, as given below:

$$\begin{aligned}\hat{\alpha}_{\rm uni} &= \frac{\alpha^2 c_3}{b} + \frac{\alpha c_2}{b} + \frac{9\alpha^2 c_7 R_s^2 \ln\left(\frac{1}{r_1}\right)}{b} \\ &+ \frac{\frac{\alpha^2 c_3}{b} + \frac{\alpha c_2}{b} + \frac{9\alpha^2 c_7 R_s^2 \ln\left(\frac{1}{r_1}\right)}{b} - \frac{12\alpha^2 c_6 R_s^2}{b} - \frac{4\alpha^2 c_7 R_s^2}{b} - \frac{\alpha^2 c_7 \ln(512) R_s^2}{b} + \frac{R_s}{b}}{1 - \frac{\omega_0^2}{\omega^2}} \\ &+ \frac{5\alpha^2 c_7 R_s^2}{b} - \frac{12\alpha^2 c_6 R_s^2}{b} - \frac{9\alpha^2 c_7 \ln(2) R_s^2}{b} + \frac{R_s}{b}.\end{aligned} \tag{38}$$

We can plot the dependence of the angle of deflection on the impact parameter b, $\frac{\omega_0^2}{\omega^2}$, α, c_2, c_3, c_6, and c_7 for various values of other parameters of $f(Q)$ gravity, such as c_2, c_3, c_6, c_7, ω_e^2/ω^2 etc in the BH spacetime of $f(Q)$ gravity. This behavior is represented graphically in figure 9. It can be seen that the deflection angle $\hat{\alpha}_{uni}$ for $f(Q)$ gravity is less than for the GR case ($\alpha = 0$).

4.2. Nonuniform plasma distribution

This part of our analysis consists of a non-singular isothermal sphere (SIS), which is the most advantageous model to understand specific properties of the photon sphere around a BH in weak gravitational lensing. In general, an SIS is a spherical gas cloud having singularity which is detected at its centre where the density leads to infinity. The distribution of density for an SIS is as follows [33]:

$$\rho(r) = \frac{\sigma_\nu^2}{2\pi r^2}, \tag{39}$$

where σ_ν^2 leads to the one-dimensional velocity dispersion. The expression below represents the plasma concentration [33]

$$N(r) = \frac{\rho(r)}{km_p}, \tag{40}$$

where m_p denotes the mass and k denotes the dimension-free constant coefficient of the dark-matter–dominated Universe. The plasma frequency in its expressive form is given below:

$$\omega_e^2 = K_e N(r) = \frac{K_e \sigma_\nu^2}{2\pi k m_p r^2}. \tag{41}$$

Here, we explain the effects of nonuniform plasma on the deflection angle in the $f(Q)$ gravity BH spacetime. Expression of the deflection angle in $f(Q)$ gravity around the BH may be written as [40]:

$$\hat{\alpha}_{SIS} = \hat{\alpha}_{SIS1} + \hat{\alpha}_{SIS2} + \hat{\alpha}_{SIS3}. \tag{42}$$

By the combination of equations (32), (36) and (42), one can get the deflection angle in the following form:

$$\begin{aligned}\hat{\alpha}_{SIS} &= \frac{6\alpha^2 c_7 \omega_c^2 R_s^4 \ln\left(\frac{1}{r_1}\right)}{\pi b^3 \omega^2} - \frac{8\alpha^2 c_6 \omega_c^2 R_s^4}{\pi b^3 \omega^2} \\ &- \frac{11\alpha^2 c_7 \omega_c^2 R_s^4}{3\pi b^3 \omega^2} + \frac{2\alpha^2 c_3 \omega_c^2 R_s^2}{3\pi b^3 \omega^2} \\ &- \frac{6\alpha^2 c_7 \ln(2) \omega_c^2 R_s^4}{\pi b^3 \omega^2} + \frac{2\alpha c_2 \omega_c^2 R_s^2}{3\pi b^3 \omega^2} + \frac{2\omega_c^2 R_s^3}{3\pi b^3 \omega^2} \\ &+ \frac{2\alpha^2 c_3}{b} + \frac{2\alpha c_2}{b} + \frac{18\alpha^2 c_7 R_s^2 \ln\left(\frac{1}{r_1}\right)}{b} + \frac{\alpha^2 c_7 R_s^2}{b} \\ &- \frac{24\alpha^2 c_6 R_s^2}{b} \\ &- \frac{9\alpha^2 c_7 \ln(2) R_s^2}{b} - \frac{\alpha^2 c_7 \ln(512) R_s^2}{b} + \frac{2R_s}{b}.\end{aligned} \tag{43}$$

These calculations lead to a supplementary plasma constant ω_c^2 which is given in the form of the following analytic expression [34]:

$$\omega_c^2 = \frac{K_e \sigma_\nu^2}{2\pi k m_p R_S^2}. \tag{44}$$

Here, equation (43) allows us to plot the dependence of the angle of deflection with different parameters of $f(Q)$ gravity, i.e. b, $\frac{\omega_c^2}{\omega^2}$, α, c_2, c_3, c_6 and c_7, for different values of other parameters of $f(Q)$ gravity, such as c_2, c_3, c_6, c_7, ω_c^2/ω^2 for the nonuniform plasma, shown in figure 10. The deflection angle $\hat{\alpha}_{SIS}$ in $f(Q)$ gravity is less than the GR case ($\alpha = 0$).

Moreover, we compare the different effects of uniform and nonuniform plasma on the angle of deflection around the BH in $f(Q)$ gravity, represented in figure 11.

5. Conclusions

We have discussed the motion of massive and massless particles around a BH in $f(Q)$ gravity and have investigated the effects of the different spacetime parameters on the motion of these particles. We have also analysed the BH shadow and weak gravitational lensing in a plasma medium in the realm backed by the $f(Q)$ gravity spacetime. It is important to mention that we have studied the $f(Q)$ BH features making comparison with the standard Schwarzschild BH of GR. Subsequently, we have fixed other small values of α to look at the impacts of $f(Q)$ gravity. We have observed that all the $f(Q)$ gravity parameters α, c_2, c_3, c_6, c_7, r_1, plasma impact parameter b, plasma distribution ω_0^2/ω^2 (*uni*) and ω_c^2/ω^2 (*SIS*) have influence on the study of the motion of particles around

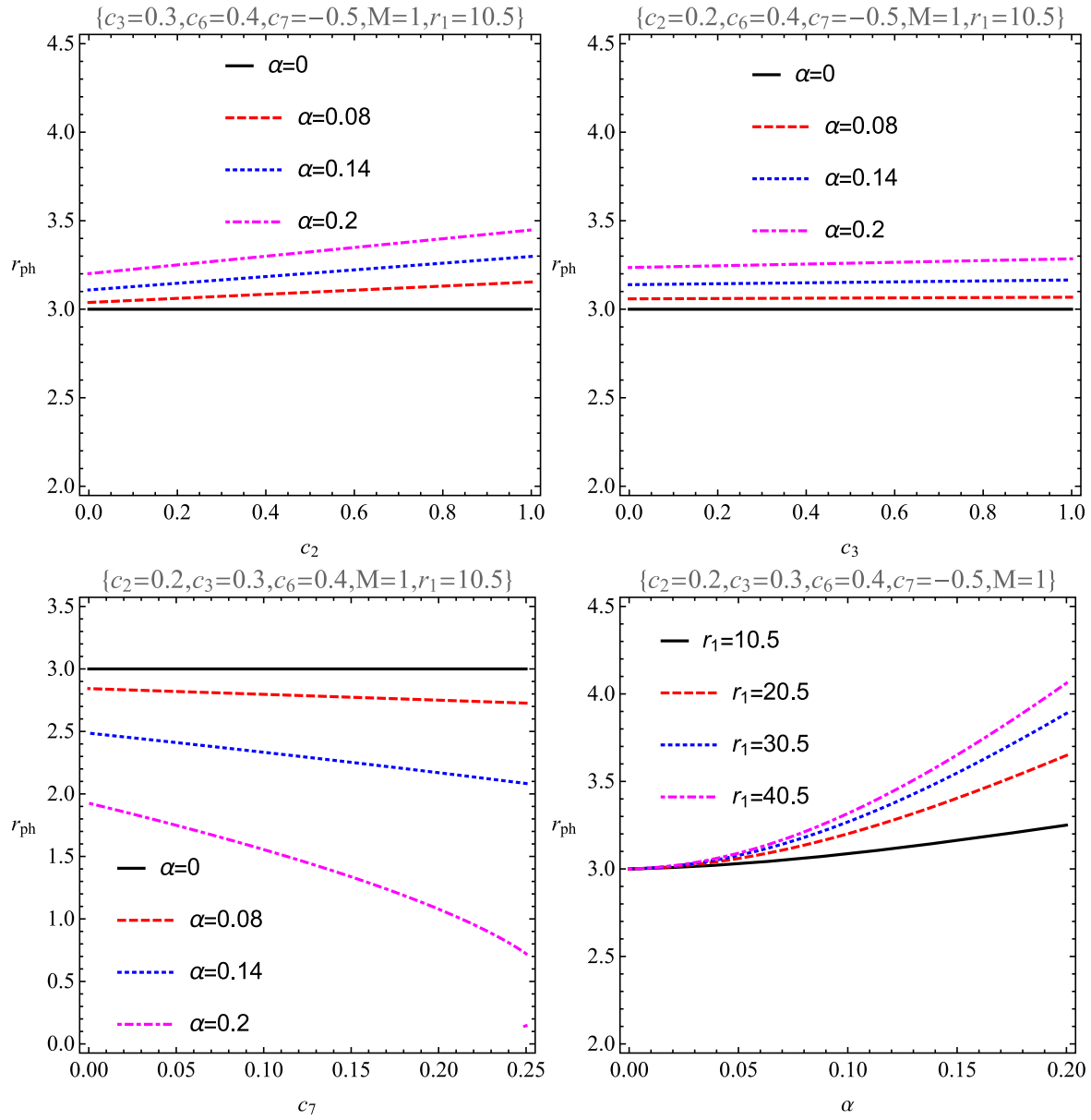

Figure 7. Radius of the photon orbit r_{ph}, with different $f(Q)$ gravity parameters for some values of α and r_1.

the BH in $f(Q)$ gravity and on the associated phenomena of gravitational lensing and shadow formation. The effects of all these $f(Q)$ gravity parameters on plasma distributions can readily be seen from the graphs in the figures. The discussion above of the dynamics of particles and the graphical analysis of the BH spacetime in $f(Q)$ gravity leads to the following concluding remarks.

- We have explored the BH horizons in the paradigm of $f(Q)$ gravity. It can be observed from figure 1 that the horizon radius increases with c_2, c_3 and α (for smaller values of α) and decreases with c_6.
- For the massive particle motion, we have studied the dependency of the effective potential on the radius r for different values of the $f(Q)$ gravity parameters as plotted in figure 2. The effective potential decreases with increasing values of α, c_2, c_3, c_7 and r_1 and increases with c_6. We have also plotted the energy $\mathcal{E}$ and angular momentum $\mathcal{L}$ in figures 3 and 4. These figures show how the energy and angular momentum of the particles change with the $f(Q)$ gravity parameters.
- We have also plotted the ISCO radius with different parameters of $f(Q)$ gravity for some values of $\alpha = 0$, 0.02, 0.04, 0.06, as shown in figure 5. We have seen that the radius of the ISCO increases with c_2 and r_1 and decreases with c_6, and c_7.
- The photon radius has been obtained in the generic way using the effective potential plotted in figure 6. We have also discussed the photon motion as plotted in figure 7. It is important to note the r_{ph} increases with c_2, c_3, r_1 and α, while it decreases with c_6, and c_7.
- Figure 8 shows the behavior of the radius of the BH shadow in $f(Q)$ gravity, which is to increase with c_2, c_3 and α but to decrease with c_6.

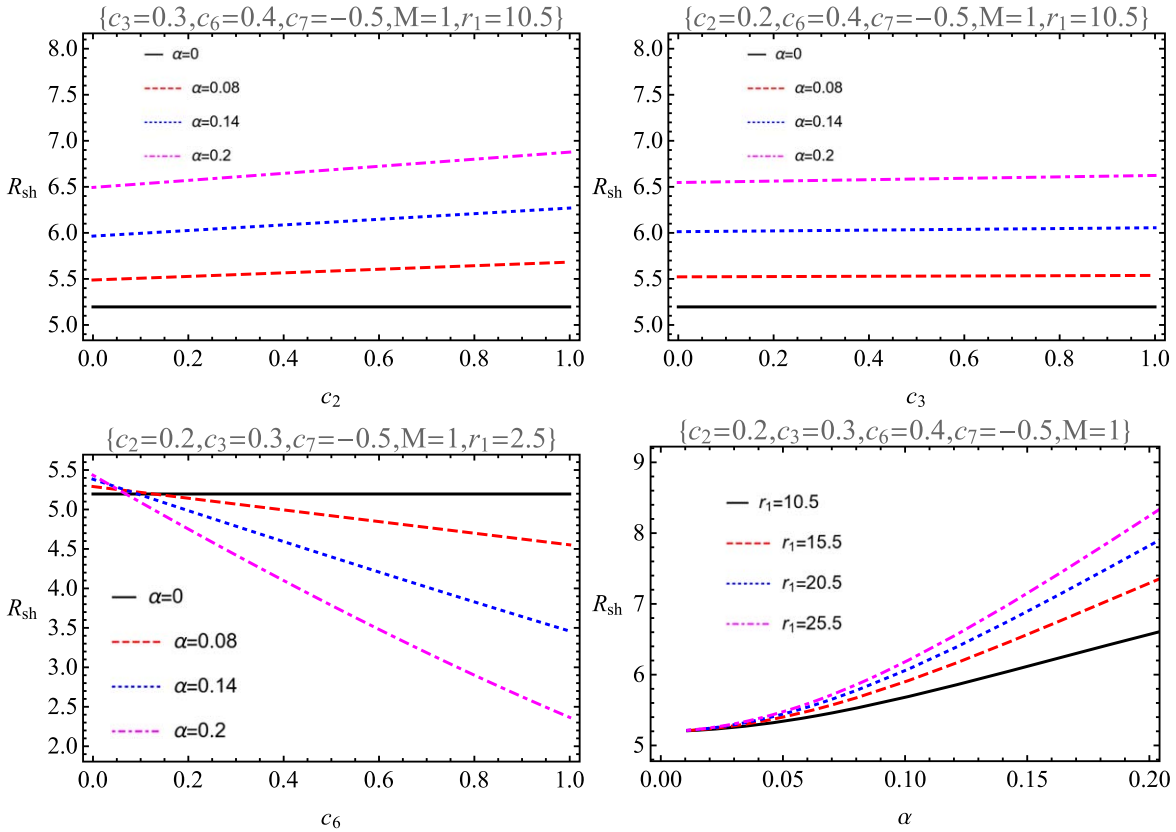

Figure 8. R_{sh} for the BH shadow with different $f(Q)$ gravity parameters for some values of α and r_1.

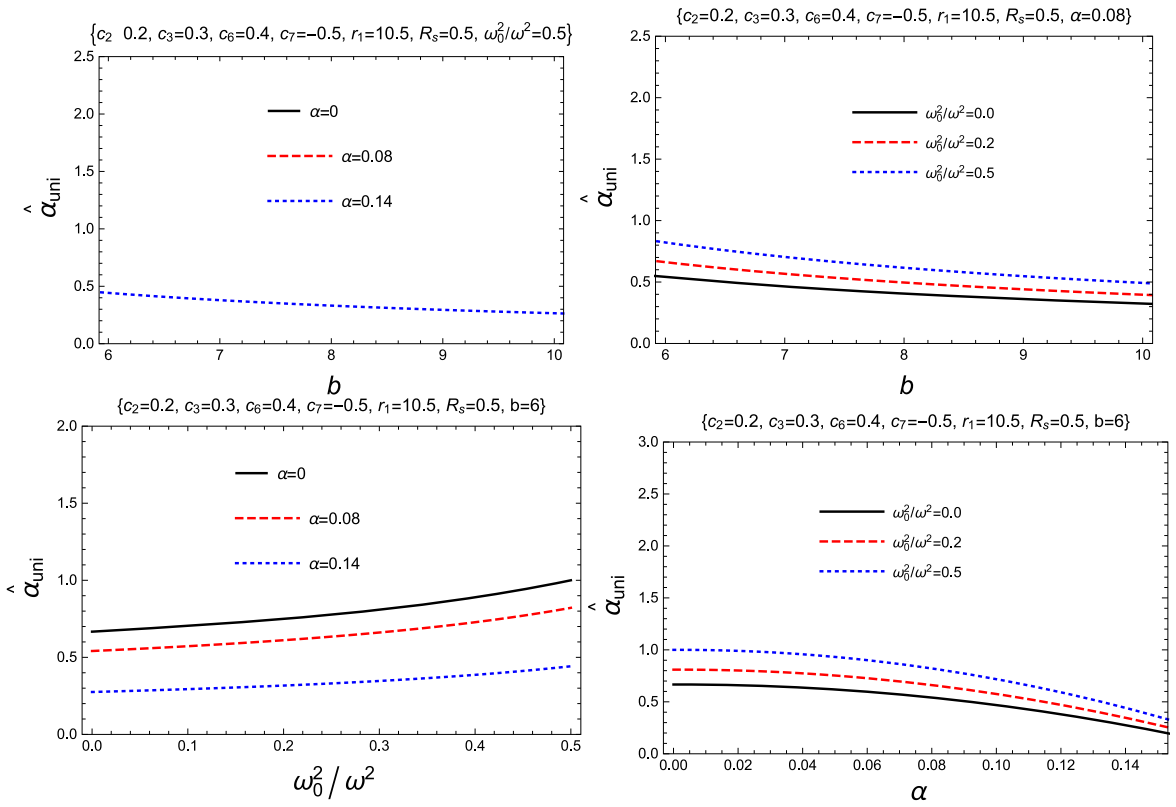

Figure 9. Uniform plasma effect with different $f(Q)$ and plasma parameters.

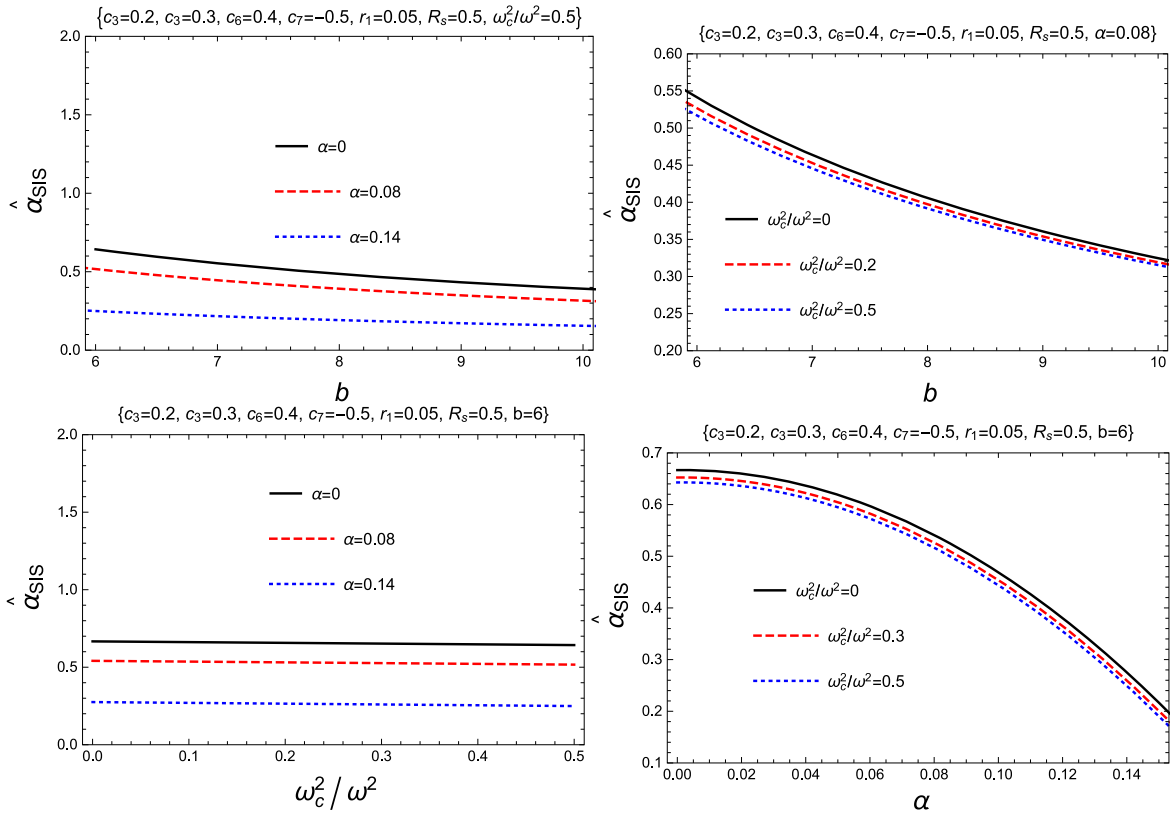

Figure 10. Nonuniform plasma effects with different $f(Q)$ and plasma parameters.

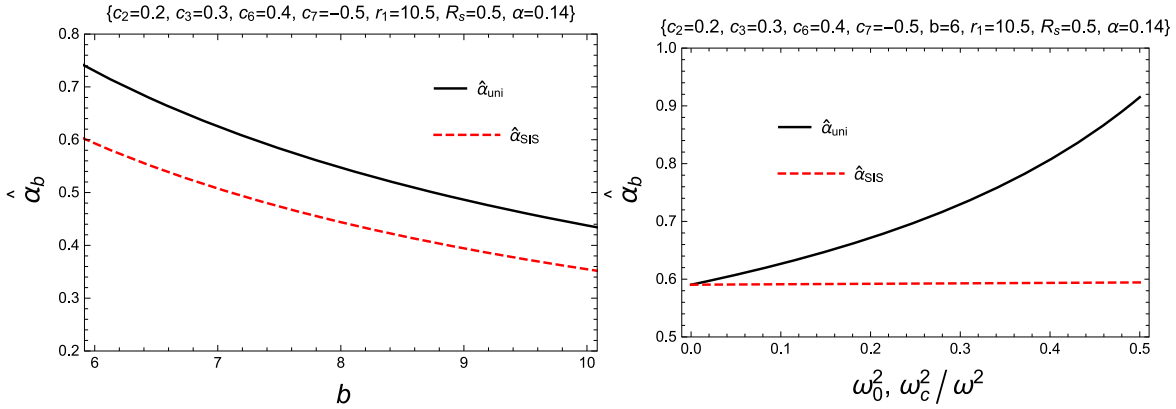

Figure 11. Difference between the different effects of uniform and nonuniform plasma in $f(Q)$ gravity.

- We have described the characteristics of the weak gravitational lensing of the BH on a light ray in $f(Q)$ gravity in uniform and nonuniform plasma concentrations, and plotted in figures 9 and 10 their increasing and decreasing effects. It is worth noting that in all the cases the concentration of uniform plasma from angle of deflection is more than the nonuniform plasma, which can be seen from figure 11.

Here we mention that this study may be of use in future related works as it contains significant new findings about the effects of the $f(Q)$ theory of gravity parameters on particle motion and associated phenomena in the BH spacetime.

Acknowledgments

This work is funded by the National Natural Science Foundation of China 11 975 145. This research is partly supported by Research Grant FZ-20200929344 and F-FA-2021-510 of the Uzbekistan Ministry for Innovative Development. G. Mustafa is very thankful to Prof. Gao Xianlong from the Department of Physics, Zhejiang Normal University, for his kind support and help during this research. Further to this, G. Mustafa acknowledges Grant No. ZC304022919 to support his Postdoctoral Fellowship at Zhejiang Normal University.

ORCID iDs

Allah Ditta https://orcid.org/0000-0001-7758-8736
Ibrar Hussain https://orcid.org/0000-0003-0733-900X

References

[1] Clifford M W 2006 The confrontation between general relativity and experiment *Living Rev. Relativ.* **9** 3
[2] Abbott B P *et al* 2016 Observation of gravitational waves from a binary black hole merger *Phys. Rev. Lett* **116** 061102
[3] Akiyama K *et al* 2019 First M87 event horizon telescope results. i. the shadow of the supermassive black hole *ApJ.* **875** L1
[4] Akiyama K *et al* 2019 First M87 event horizon telescope results. vi. the shadow and mass of the central black hole *Astrophys. J.* **875** L6
[5] Jiménez J B, Heisenberg L and Koivisto T 2018 Coincident general relativity *Phys. Rev.* D **98** 044048
[6] Jiménez J B, Heisenberg L and Koivisto T S 2018 Teleparallel Palatini theories *J. Cosmol. Astropart. Phys.* **2018** 039
[7] Heisenberg L 2019 A systematic approach to generalisations of general relativity and their cosmological implications *Phys. Rept.* **796** 1–113
[8] Jiménez J B, Heisenberg L and Koivisto T S 2019 The geometrical trinity of gravity *Universe* **5** 173
[9] D'Ambrosio F, Garg M, Heisenberg L and Zentarra S 2020 ADM formulation and Hamiltonian analysis of coincident general relativity arXiv:2007.03261
[10] D'Ambrosio F and Heisenberg L 2021 Classification of primary constraints of quadratic non-metricity theories of gravity *J. High Energy Phys.* **2021** 170
[11] Jiménez J B, Heisenberg L, Koivisto T and Pekar S 2020 Cosmology in f (Q) geometry *Phys. Rev.* D **101** 103507
[12] Zhao D 2022 Covariant formulation of f(Q) theory *Eur. Phys. J.* C **82** 303
[13] Lin R-H and Zhai X-H 2021 Spherically symmetric configuration in f (Q) gravity *Phys. Rev.* D **103** 124001
[14] D'Ambrosio F, Fell S D B, Heisenberg L and Kuhn S 2022 Black holes in f (Q) gravity *Phys. Rev.* D **105** 024042
[15] Jawad A, Ali F, Shahzad M U and Abbas G 2016 Dynamics of particles around time conformal Schwarzschild black hole *Eur. Phys. J.* C **76** 586
[16] Teo E 2003 Spherical photon orbits around a Kerr black hole *Gen. Relativ. Gravitation* **35** 1909–26
[17] Zaslavskii O B 2012 Acceleration of particles near the inner black hole horizon *Phys. Rev.* D **85** 024029
[18] Narzilloev B, Shaymatov S, Hussain I, Abdujabbarov A, Ahmedov B and Bambi C 2021 Motion of particles and gravitational lensing around the (2.1)-dimensional BTZ black hole in Gauss-Bonnet gravity *Eur. Phys. J.* C **81** 849
[19] Turimov B, Rayimbaev J, Abdujabbarov A, Ahmedov B and Stuchlík Z 2020 Test particle motion around a black hole in Einstein-Maxwell-scalar theory *Phys. Rev.* D **102** 064052
[20] Gralla S E, Porfyriadis A P and Warburton N 2015 Particle on the innermost stable circular orbit of a rapidly spinning black hole *Phys. Rev.* D **92** 064029
[21] Jefremov P I, Tsupko O Y and B-K G S 2015 Innermost stable circular orbits of spinning test particles in Schwarzschild and Kerr space-times *Phys. Rev.* D **91** 124030
[22] Chakraborty C and Bhattacharyya S 2019 Circular orbits in Kerr-Taub-NUT spacetime and their implications for accreting black holes and naked singularities *J. Cosmol. Astropart. Phys.* **2019** 034
[23] Shaymatov S and Atamurotov F 2021 Geodesic circular orbits sharing the same orbital frequencies in the black string spacetime *Galaxies* **9** 40
[24] Atamurotov F, Shaymatov S and Ahmedov B 2021 Particle motion and plasma effects on gravitational weak lensing in lorentzian wormhole spacetime *Galaxies* **9** 54
[25] Hackmann E, Nandan H and Sheoran P 2020 Particle collisions near static spherically symmetric black holes *Phys. Lett.* B **810** 135850
[26] Abdujabbarov A, Ahmedov B and Ahmedov B 2011 Energy extraction and particle acceleration around a rotating black hole in Hořava-Lifshitz gravity *Phys. Rev.* D **84** 044044
[27] Bokhari A H, Rayimbaev J and Ahmedov B 2020 Test particles dynamics around deformed Reissner-Nordström black hole *Phys. Rev.* D **102** 124078
[28] Narzilloev B, Rayimbaev J, Shaymatov S, Abdujabbarov A, Ahmedov B and Bambi C 2020 Dynamics of test particles around a Bardeen black hole surrounded by perfect fluid dark matter *Phys. Rev.* D **102** 104062
[29] Stuchlík Z, Blaschke M and Schee J 2017 Particle collisions and optical effects in the mining Kerr-Newman spacetimes *Phys. Rev.* D **96** 104050
[30] Toshmatov B, Abdujabbarov A, Ahmedov B and Stuchlík Z 2015 Particle motion and Penrose processes around rotating regular black hole *Astrophys. Space. Sci.* **357** 41
[31] Bartelmann M and Schneider P 2001 Weak gravitational lensing *Phys. Rep.* **340** 291–472
[32] Schneider P and Weiss A 1987 A gravitational lens origin for AGN-variability? Consequences of micro- lensing *Astron. Astrophys.* **171** 49–65
[33] B-K G S and Tsupko O Y 2010 Gravitational lensing in a non-uniform plasma *Mon. Not. R. Astron. Soc.* **404** 1790
[34] Babar G Z, Atamurotov F and Babar A Z 2021 Gravitational lensing in 4-D Einstein-Gauss-Bonnet gravity in the presence of plasma *Physics of the Dark Universe* **32** 100798
[35] Atamurotov F, Sarikulov F, Abdujabbarov A and Ahmedov B 2022 Gravitational weak lensing by black hole in Horndeski gravity in presence of plasma *Eur. Phys. J. Plus* **137** 336
[36] Ditta A, Tiecheng X, Atamurotov F, Mustafa G and Abdujabbarov A 2023 Testing metric-affine gravity using particle dynamics and photon motion *Physics of the Dark Universe* **41** 101248
[37] Atamurotov F, Abdujabbarov A and Han W-B 2021 Effect of plasma on gravitational lensing by a Schwarzschild black hole immersed in perfect fluid dark matter *Phys. Rev.* D **104** 084015
[38] Hakimov A and Atamurotov F 2016 Gravitational lensing by a non-Schwarzschild black hole in a plasma *Astrophys. Space. Sci.* **361** 112
[39] Atamurotov F, Shaymatov S, Sheoran P and Siwach S 2021 Charged black hole in 4D Einstein-Gauss-Bonnet gravity: particle motion, plasma effect on weak gravitational lensing and centre-of-mass energy *J. Cosmol. Astropart. Phys.* **2021** 045
[40] Atamurotov F, Abdujabbarov A and Rayimbaev J 2021 Weak gravitational lensing Schwarzschild-MOG black hole in plasma *Eur. Phys. J.* C **81** 118
[41] B-G C A, Abdujabbarov A A and Bambi C 2018 Gravitational lensing for a boosted Kerr black hole in the presence of plasma *Eur. Phys. J.* C **78** 694
[42] Rogers A 2015 Frequency-dependent effects of gravitational lensing within plasma *Mon. Not. R. Astron. Soc.* **451** 17
[43] Er X and Mao S 2014 Effects of plasma on gravitational lensing *Mon. Not. R. Astron. Soc.* **437** 2180–6
[44] Babar G Z, Atamurotov F, Islam S U and Ghosh S G 2021 Particle acceleration around rotating Einstein-Born-Infeld black hole and plasma effect on gravitational lensing *Phys. Rev.* D **103** 084057
[45] Atamurotov F, Ortiqboev D, Abdujabbarov A and Mustafa G 2022 Particle dynamics and gravitational weak lensing around black hole in the Kalb-Ramond gravity *Eur. Phys. J.* C **82** 659

[46] Atamurotov F and Ghosh S G 2022 Gravitational weak lensing by a naked singularity in plasma *Eur. Phys. J. Plus* **137** 662

[47] Atamurotov F, Hussain I, Mustafa G and Övgün A 2023 Weak deflection angle and shadow cast by the charged-Kiselev black hole with cloud of strings in plasma *Chin. Phys.* C **47** 025102

[48] Atamurotov F, Alibekov H, Abdujabbarov A, Mustafa G and Aripov M M 2023 Weak gravitational lensing around Bardeen black hole with a string cloud in the presence of plasma *Symmetry* **15** 848

[49] Atamurotov F, Alloqulov M, Abdujabbarov A and Ahmedov B 2022 Testing the Einstein-Æther gravity: particle dynamics and gravitational lensing *Eur. Phys. J. Plus* **137** 634

[50] Atamurotov F, Sarikulov F, Khamidov V and Abdujabbarov A 2022 Gravitational weak lensing of Schwarzschild-like black hole in presence of plasma *Eur. Phys. J. Plus* **137** 567

[51] Liu F-Y, Mai Y-F, Wu W-Y and Xie Y 2019 Probing a regular non-minimal Einstein-Yang-Mills black hole with gravitational lensings *Phys. Lett.* B **795** 475–81

[52] Lu X and Xie Y 2019 Weak and strong deflection gravitational lensing by a renormalization group improved Schwarzschild black hole *Eur. Phys. J. C* **79** 1016

[53] Wang C-Y, Shen Y-F and Xie Y 2019 Weak and strong deflection gravitational lensings by a charged Horndeski black hole *J. Cosmol. Astropart. Phys.* **2019** 022

[54] Gao Y-X and Xie Y 2021 Gravitational lensing by hairy black holes in Einstein-scalar-Gauss-Bonnet theories *Phys. Rev.* D **103** 043008

[55] Landau L D, Bell J S, Kearsley M J, Pitaevskii L P, Lifshitz E M and Sykes J B 2013 *Electrodynamics of Continuous Media* (Amsterdam: Elsevier)

[56] Muhleman D O, Ekers R D and Fomalont E B 1970 Radio interferometric test of the general relativistic light bending near the sun *Phys. Rev. Lett.* **24** 1377–80

[57] Lightman A P, Press W H, Price R H and Teukolsky S A 1979 *Problem Book in Relativity and Gravitation* (Princeton, NJ: Princeton University Press)

[58] Cunha P V P and Herdeiro C A R 2018 Shadows and strong gravitational lensing: a brief review *Gen. Relativ. Gravit.* **50** 42

[59] Cunha P V P, Eiró N A, Herdeiro C A R and Lemos J P S 2020 Lensing and shadow of a black hole surrounded by a heavy accretion disk *J. Cosmol. Astropart. Phys.* **2020** 035

[60] Falcke H, Melia F and Agol E 2000 Viewing the shadow of the black hole at the galactic center *Astrophys. J.* **528** L13–6

[61] Perlick V and Tsupko O Y 2022 Calculating black hole shadows: Review of analytical studies *Phys. Rep.* **9 947** 1–39

[62] Atamurotov F, Papnoi U and Jusufi K 2022 Shadow and deflection angle of charged rotating black hole surrounded by perfect fluid dark matter *Classical Quantum Gravity* **39** 025014

[63] Papnoi U and Atamurotov F 2022 Rotating charged black hole in 4 D Einstein-Gauss-Bonnet gravity: Photon motion and its shadow *Physics of the Dark Universe* **35** 100916

[64] Atamurotov F, Abdujabbarov A and Ahmedov B 2013 Shadow of rotating non-Kerr black hole *Phys. Rev.* D **88** 064004

[65] Abdujabbarov A, Atamurotov F, Kucukakca Y, Ahmedov B and Camci U 2013 Shadow of Kerr-Taub-NUT black hole *Astrophys. Space. Sci.* **344** 429–35

[66] Atamurotov F, Abdujabbarov A and Ahmedov B 2013 Shadow of rotating Hořava-Lifshitz black hole *Astrophys. Space. Sci.* **348** 179–88

[67] Papnoi U, Atamurotov F, Ghosh S G and Ahmedov B 2014 Shadow of five-dimensional rotating Myers-Perry black hole *Phys. Rev.* D **90** 024073

[68] Abdujabbarov A, Atamurotov F, Dadhich N, Ahmedov B and Stuchlík Z 2015 Energetics and optical properties of 6-dimensional rotating black hole in pure Gauss-Bonnet gravity *Eur. Phys. J.* C **75** 399

[69] Atamurotov F, Ghosh S G and Ahmedov B 2016 Horizon structure of rotating Einstein-Born-Infeld black holes and shadow *Eur. Phys. J.* C **76** 273

[70] Abdujabbarov A, Ahmedov B, Dadhich N and Atamurotov F 2017 Optical properties of a braneworld black hole: Gravitational lensing and retrolensing *Phys. Rev. D.* **96** 084017

[71] G-N M, A-A M, Jusufi K and Jamil M 2020 Shadow, quasinormal modes, and quasiperiodic oscillations of rotating Kaluza-Klein black holes *Phys. Rev. D* **102** 104032

[72] Afrin M, Kumar R and Ghosh S G 2021 Parameter estimation of hairy Kerr black holes from its shadow and constraints from M87* *Mon. Not. R. Astron. Soc.* **504** 5927–40

[73] Okyay M and Övgün A 2022 Nonlinear electrodynamics effects on the black hole shadow, deflection angle, quasinormal modes and greybody factors *J. Cosmol. Astropart. Phys.* **01** 009

[74] Pantig R C, Yu P K, Rodulfo E T and Övgün A 2022 Shadow and weak deflection angle of extended uncertainty principle black hole surrounded with dark matter *Ann. Phys.* **436** 168722

[75] Övgün A and Sakallı İ 2020 Testing generalized Einstein–Cartan–Kibble–Sciama gravity using weak deflection angle and shadow cast *Class. Quant. Grav.* **37** 225003

[76] Övgün A, Sakallı İ and Saavedra J 2018 Shadow cast and deflection angle of Kerr-Newman-Kasuya spacetime *J. Cosmol. Astropart. Phys.* **10** 041

[77] Vagnozzi S *et al* 2023 Horizon-scale tests of gravity theories and fundamental physics from the Event Horizon Telescope image of Sagittarius A* *Class. Quantum Grav.* **40** 165007

[78] Sarikulov F, Atamurotov F, Abdujabbarov A and Ahmedov B 2022 Shadow of the Kerr-like black hole *Eur. Phys. J.* C **82** 771

[79] Mustafa G, Atamurotov F, Hussain I, Shaymatov S and Övgün A 2022 Shadows and gravitational weak lensing by the Schwarzschild black hole in the string cloud background with quintessential field *Chin. Phys.* C **46** 125107

[80] Farruh Atamurotov I H, Mustafa G and Jusufi K 2022 Shadow and quasinormal modes of the Kerr-Newman-Kiselev-Letelier black hole *Eur. Phys. J.* C **82** 831

[81] Perlick V, Tsupko O Y and B-K G S 2015 Influence of a plasma on the shadow of a spherically symmetric black hole *Phys. Rev.* D **92** 104031

[82] Perlick V and Tsupko O Y 2017 Light propagation in a plasma on Kerr spacetime: Separation of the Hamilton-Jacobi equation and calculation of the shadow *Phys. Rev.* D **95** 104003

[83] Atamurotov F, Jusufi K, Jamil M, Abdujabbarov A and A-A M 2021 Axion-plasmon or magnetized plasma effect on an observable shadow and gravitational lensing of a Schwarzschild black hole *Phys. Rev.* D **104** 064053

[84] Badía J and Eiroa E F 2021 Shadow of axisymmetric, stationary, and asymptotically flat black holes in the presence of plasma *Phys. Rev.* D **104** 084055

[85] Atamurotov F, Ahmedov B and Abdujabbarov A 2015 Optical properties of black holes in the presence of a plasma: The shadow *Phys. Rev.* D **92** 084005

[86] Babar G Z, Babar A Z and Atamurotov F 2020 Optical properties of Kerr-Newman spacetime in the presence of plasma *Eur. Phys. J.* C **80** 761

[87] Chowdhuri A and Bhattacharyya A 2021 Shadow analysis for rotating black holes in the presence of plasma for an expanding universe *Phys. Rev.* D **104** 064039

[88] Fathi M, Olivares M and Villanueva J R 2021 Analytical study of light ray trajectories in Kerr spacetime in the presence of an inhomogeneous anisotropic plasma *Eur. Phys. J.* C **81** 987

[89] Melia F and Falcke H 2000 The supermassive black hole at the galactic center *Annu. Rev. Astron. Astrophys.* **39** 305–52

[90] Bronzwaer T and Falcke H 2021 The nature of black hole shadows *Astrophys. J.* **920** 155

[91] Chandrasekhar S 1998 *The Mathematical Theory of Black Holes* (Oxford: Oxford University Press)